Operational thermal remote sensing and lava flow monitoring at the Hawaiian Volcano Observatory

M. R. PATRICK[1]*, J. KAUAHIKAUA[1], T. ORR[1], A. DAVIES[2] & M. RAMSEY[3]

[1]*US Geological Survey – Hawaiian Volcano Observatory, PO Box 51, Hawaii National Park, Hawai'i, HI 96718, USA*

[2]*NASA Jet Propulsion Laboratory, 4800 Oak Grove Drive, Pasadena, CA 91109, USA*

[3]*Department of Geology and Planetary Science, University of Pittsburgh, 4107 O'Hara Street, Pittsburgh, PA 15260, USA*

**Corresponding author (e-mail: mpatrick@usgs.gov)*

Abstract: Hawaiian volcanoes are highly accessible and well monitored by ground instruments. Nevertheless, observational gaps remain and thermal satellite imagery has proven useful in Hawai'i for providing synoptic views of activity during intervals between field visits. Here we describe the beginning of a thermal remote sensing programme at the US Geological Survey Hawaiian Volcano Observatory (HVO). Whereas expensive receiving stations have been traditionally required to achieve rapid downloading of satellite data, we exploit free, low-latency data sources on the internet for timely access to GOES, MODIS, ASTER and EO-1 ALI imagery. Automated scripts at the observatory download these data and provide a basic display of the images. Satellite data have been extremely useful for monitoring the ongoing lava flow activity on Kīlauea's East Rift Zone at Pu'u 'Ō'ō over the past few years. A recent lava flow, named Kahauale'a 2, was upslope from residential subdivisions for over a year. Satellite data helped track the slow advance of the flow and contributed to hazard assessments. Ongoing improvement to thermal remote sensing at HVO incorporates automated hotspot detection, effusion rate estimation and lava flow forecasting, as has been done in Italy. These improvements should be useful for monitoring future activity on Mauna Loa.

Hawai'i's active volcanoes are among the best monitored and most accessible on Earth. Instrumentation on Mauna Loa and Kīlauea volcanoes, the most active in Hawai'i in historic times, includes arrays of seismometers, GPS, tiltmeters, gas sensors, strainmeters and webcams (Guffanti *et al.* 2009). Areas of ongoing eruptive activity are relatively close to populated areas, and those spots that cannot be accessed by car or on foot can usually be reached in a relatively short helicopter ride. Nevertheless, significant observational gaps remain. For instance, active lava flows in remote areas of the volcano might not be easily imaged by our field webcams, in part owing to the low slopes on these shield volcanoes and highly oblique camera viewing angles. Remote surface activity like this would then require periodic field visits via helicopter. Continuing federal budget cuts have reduced the frequency of helicopter overflights, making it more difficult to directly access remote lava flows.

Satellite remote sensing is a natural solution to fill these observational gaps in Hawai'i. Satellite imagery is acquired at regular intervals and provides a synoptic view of the volcano, imaging remote activity easily. The effectiveness of satellite imagery for volcano monitoring has been demonstrated in the scientific literature over the past few decades (see review in Harris 2013). Operational volcano monitoring, however, has several critical requirements for remote sensing data, one of which is low latency (i.e. minimal time between acquisition at the satellite and availability at the observatory). Traditionally, this low latency requirement has been satisfied through the use of receiving stations that directly download data from the satellites, often resulting in latency of just minutes. Such receiving stations, however, are very expensive to purchase and require significant resources to maintain. The recent availability of relatively low-latency satellite data over the internet, however, now provides an opportunity for operational monitoring – to a limited degree – without the need for a satellite receiving station.

In this methodology paper we describe a nascent thermal remote sensing programme at the Hawaiian Volcano Observatory (HVO), using data automatically downloaded from the internet. This paper describes the first stage of this programme, which

From: Harris, A. J. L., De Groeve, T., Garel, F. & Carn, S. A. (eds) *Detecting, Modelling and Responding to Effusive Eruptions*. Geological Society, London, Special Publications, **426**, http://doi.org/10.1144/SP426.17

tackles data acquisition and display. We show how the satellite data complemented our field observations for monitoring the advancement of the Kahauale'a 2 lava flow on Kīlauea's East Rift Zone during 2013–2014. Ongoing work at HVO focuses on implementing automated routines for alarming and analysis, as has been done at in Italy.

Background

Hawai'i has three subaerial volcanoes (Kīlauea, Mauna Loa, Hualālai) that have erupted in the historic period (i.e. since about AD 1800; Fig. 1). Kīlauea Volcano is currently erupting at two locations, the summit and the East Rift Zone. The summit eruption began in March 2008 and now consists of a large lava lake contained within Halema'uma'u Crater, in the summit caldera (Patrick *et al.* 2013). The East Rift Zone eruption, focused around Pu'u 'Ō'ō cone 18.5 km to the ESE, began in 1983 with episodes of high lava fountaining that changed into steady effusion by the late 1980s (Heliker & Mattox 2003). The activity since that time has largely consisted of tube-fed pāhoehoe flows that have migrated south to reach the ocean (Orr *et al.* 2013). Since January 2013, Pu'u 'Ō'ō lava flows have followed a northeasterly route, which is unusual, but not unprecedented (Kauahikaua 2007), for the Pu'u 'Ō'ō flow field. During 2013 to mid-2014, lava was feeding the Kahauale'a 2 flow. The northeasterly direction put the flow upslope of several large residential subdivisions in the Puna district, and was an ongoing hazard concern during 2013–2014.

Mauna Loa's most recent eruption was in 1984, during which lava flows stalled approximately 7 km from the outskirts of Hilo (pop. 43 000) (Lockwood *et al.* 1987). Inflation and increased seismic activity on Mauna Loa during 2002–2004 suggested reawakening but did not lead to an eruption (Miklius & Cervelli 2003; Miklius *et al.* 2005; Amelung *et al.* 2007). The current repose period, of over 30 years, is the longest eruption interval in Mauna Loa's historic record.

Hualālai Volcano's most recent eruption was in 1801, producing a lava flow that reached the ocean at the current site of the Kona International Airport (Kauahikaua *et al.* 2002). A major seismic swarm in 1929 (Jaggar 1930) may have been due to a 'failed' eruption (i.e. magma migrating upwards without reaching the surface; Macdonald 1954, see also Moran *et al.* 2011). Increased tourism and development on the lower slopes of Hualālai mean that

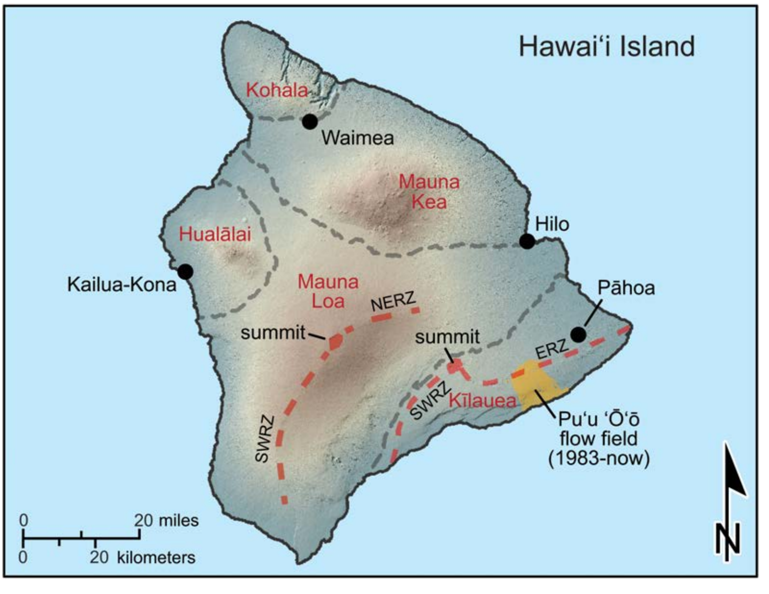

Fig. 1. Hawai'i is the southernmost island in the Hawaiian chain, and contains three volcanoes that have erupted during historic times (since about AD 1800): Hualālai (most recent eruption 1801), Mauna Loa (most recent eruption 1984) and Kīlauea (two ongoing eruptions). Kīlauea is erupting at the summit, where there is a lava lake in Halema'uma'u Crater, and along the East Rift Zone (ERZ), focused around Pu'u 'Ō'ō. The Pu'u 'Ō'ō eruption began in 1983, and has produced the lava flow field shown by the orange area (as mapped in 2013). Kīlauea also has a Southwest Rift Zone (SWRZ). Mauna Loa's eruptions typically occur at the summit or along one of its rift zones (the Northeast Rift Zone, NERZ, or Southwest Rift Zone, SWRZ). Selected towns are shown by black dots.

future eruptions will probably have very high risk potential.

The frequent activity on Kīlauea has made it a natural target for thermal remote sensing studies (see review in Harris 2013; also bibliography in Heliker & Mattox 2003). One of the first demonstrations of thermal satellite data for volcano monitoring, in fact, was at Kīlauea Volcano in 1964 (Gawarecki *et al.* 1965; Harris 2013). The Gawarecki study illustrated how lava flows can create a conspicuous anomaly in thermal satellite images – data that were otherwise intended to monitor weather. The long-term eruption at Pu'u 'Ō'ō on the East Rift Zone, and the increasing quality and accessibility of thermal satellite data, led to an increase in the number of studies in the 1990s. Flynn *et al.* (1994) used Landsat data to delineate regions of activity on the Pu'u 'Ō'ō flow field, discriminating between lava tube, a lava lake and active surface flows. Harris *et al.* (1998) also used Landsat data at Kīlauea, and estimated lava effusion rates based on the nature of the thermal anomalies. Harris *et al.* (1997*a*) and Harris & Thornber (1999) were some of the first studies to take advantage of the high temporal resolution of GOES (Geostationary Operational Environmental) data for tracking dynamic volcanic activity. This was followed by Harris *et al.* (2001), who published GOES results for Kīlauea on the internet. Wright *et al.* (2002, 2004) developed an automated worldwide thermal alert system (MODVOLC) based on MODIS (Moderate Resolution Imaging Spectroradiometer) imagery, with Kīlauea's East Rift Zone lava flow field acting as a major test case. More recent work by Koeppen *et al.* (2011) refined the MODVOLC system with regionally tailored sensitivities that increased detection accuracy, again using Kīlauea's flow field as a test case. Patrick & Witzke (2011) used ASTER data to map thermal areas on Mauna Loa and Kīlauea. Koeppen *et al.* (2013) analysed 10 years of MODIS data over Kīlauea's flow field and compared the radiant heat flux trends with sulfur dioxide emission rates and field observations to determine the partitioning of lava between lava tubes and surface breakouts.

While research using thermal satellite data has been plentiful, operational use of thermal remote sensing data at HVO has been limited until recently. Much of the difficulty has been obtaining satellite data within a reasonable time frame. The latency requirements at HVO are based on the primary hazard, which is from lava flows. At Kīlauea, these lava flows have generally been slow moving (at most several hundreds of metres per day), and thus the latency of satellite data need not be as short as for, say, explosive eruptions whose hazards might change over minutes. Nevertheless, information on lava flow activity is of limited use at HVO if the data are much older than a day – in part because HVO releases a daily update on the ongoing eruptive activity. With no receiving station, HVO has not had direct access to low-latency satellite imagery until recently. Ease of access has been another limiting issue. The time required to manually search for new images online, download and then process them may be prohibitive for a small observatory with many other obligations and urgencies. Thus, automating all, or nearly all, of the process is absolutely essential in an operational monitoring environment.

Satellite data sources and analyses

GOES

The GOES-15 satellite is operated by the United States NOAA (National Oceanographic and Atmospheric Administration) and is positioned to image the Western Hemisphere, providing an image every 15 min. The high temporal resolution is at the expense of spatial resolution, with visual images having a pixel size of 1 km at the equator, and infrared images having a pixel size of 4 km at the equator.

Given the high temporal resolution, the GOES satellite is well suited to identifying the onset of new eruptive activity or rapid changes in the intensity of ongoing activity (Harris *et al.* 1997*a*, 2001). The low spatial resolution means that the precise location and distribution of such activity cannot be determined. Nevertheless, temporal constraints on activity are of fundamental importance in operational monitoring. Following Harris *et al.* (1997*a*, 2001), we focus on using Band 2 data (3.9 μm). These shortwave infrared data are particularly sensitive to high-temperature surfaces, and thus provide clear identification of effusive activity (Fig. 2a). In practice at HVO, GOES data are useful during brief decreases in activity to check whether surface breakouts have diminished or disappeared. The data would be particularly useful, however, to identify new activity during the next eruption of Mauna Loa. In other words, the GOES data are of limited use during continuous eruptions but are of significant importance in detecting the start of new eruptions.

Near-real-time GOES data are available for downloading at the NASA (United States National Aeronautics and Space Administration) Goddard Space Flight Center. The FTP site is available via http://goes.gsfc.nasa.gov, and data are available in sectors, one of which is Hawai'i. A Matlab (version 2012a®, The Mathworks Inc.) script is run every 10 min via Windows Scheduler and checks the NASA FTP site for new images, based on the

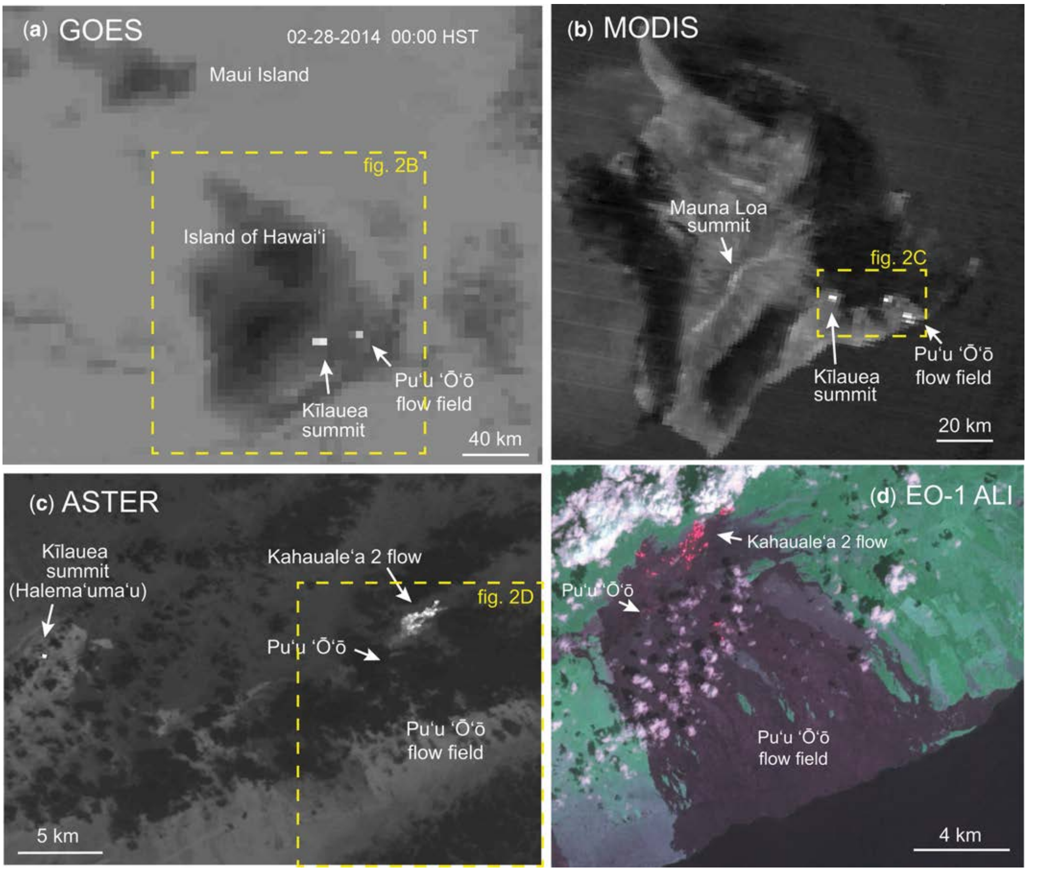

Fig. 2. Selected images of the four data types (GOES, MODIS, ASTER and EO-1 ALI) that are automatically downloaded and processed at the Hawaiian Volcano Observatory. Yellow boxes show the extent of the labelled subfigure. (**a**) GOES image (Band 2, 4 µm) from 28 February 2014, showing Maui and Hawai'i Islands. Two thermal anomalies are present, one at the summit and one on the Pu'u 'Ō'ō flow field. (**b**) A MODIS Band 22 (3.9 µm) image from 1 August 2013, showing Hawai'i Island. A distinct thermal anomaly is present at the summit of Kīlauea Volcano, where a large lava lake is active. Two adjacent thermal anomalies are present on the East Rift Zone, on the Pu'u 'Ō'ō flow field. The northern anomaly corresponds to activity within Pu'u 'Ō'ō crater, and the southern anomaly represents pāhoehoe lava flows near the coast. (**c**) ASTER image (Band 14, 11 µm) from 19 January 2014, spanning from the summit of Kīlauea, where a thermal anomaly results from the lava lake, to the East Rift Zone and the Pu'u 'Ō'ō flow field. An area of elevated temperatures is present at the distal end of the Kahauale'a 2 flow, where there are active breakouts. The coverage of Figure 2d extends off the east edge of this image. (**d**) EO-1 ALI composite image (Bands 10-8-9 RGB) on 19 October 2013, showing the Pu'u 'Ō'ō flow field. Along the northern margin of the flow field, the Kahauale'a 2 flow was active in 2013–2014. The active breakouts are visible as bright red pixels, owing to the large Band 10 (2 µm) signal.

time stamp in the individual file names. The script then applies the 'Mode A' counts to Kelvin temperature conversion (http://goes.gsfc.nasa.gov/text/imager.calibration.html), and grids the data based on latitude and longitude information available in a navigational file. Images are then exported to JPEG and displayed on the HVO internal webserver, with a script also automatically constructing time-lapse movies of the individual images for each day.

In addition to simple downloading and display, the script also performs a simple temperature analysis. It divides Hualālai, Mauna Loa and Kīlauea into regions based on their summits and rift zones. For each region, the script calculates the maximum temperature and the 'background' temperature – in this case estimated as the median. This allows maximum temperature to be plotted above background through time.

MODIS

The MODIS sensor (Barnes *et al.* 1998) is operated by NASA and is on two polar orbiting satellites, Aqua and Terra. Each acquires two images per day over a given spot on the Earth, resulting in a total of four acquisitions per day (Wright *et al.* 2002). Visual bands have pixel size of 250 m, with the infrared bands at 1 km pixel size (Barnes *et al.* 1998). Given the abundance and free access, MODIS has been frequently used to monitor volcanic activity around the world (Wright & Flynn 2004; Rothery *et al.* 2005; Harris & Ripepe 2007; Kervyn *et al.* 2008), and has been bolstered by automated global detection routines for volcanic hotspots, such as MODVOLC (Wright *et al.* 2004). MODVOLC data have been particularly useful for monitoring volcanoes with limited or no ground-based instruments (e.g. Patrick & Smellie 2013).

The NASA LANCE system (http://lance-modis.eosdis.nasa.gov) provides near-real-time MODIS data via FTP download. The LANCE data have only preliminary radiometric and geographic corrections, but at fairly low latency – normally a few hours after acquisition. In our system, a Matlab script is run by Windows Scheduler each hour and checks the LANCE FTP site for new images over Hawaiʻi Island, by scanning the metadata files for geographic coordinates that cover Hawaiʻi. If a new image is available, the script downloads the image. A second script then takes the Band 22 (3.9 μm) data and warps it to a UTM (Universal Transverse Mercator) projection for display, exporting the image as a JPEG file that is available on the HVO internal website (Fig. 2b).

ASTER

ASTER (Advanced Spaceborne Thermal Emission and Reflection Radiometer) is a joint USA–Japan polar-orbiting sensor on the NASA Terra satellite that provides visible and thermal infrared channels at pixel sizes of 15 and 90 m, respectively (Yamaguchi *et al.* 1998; Pieri & Abrams 2004). The instrument previously provided several shortwave infrared bands, but that detector went offline in April 2008. Repeat periods for ASTER over Hawaiʻi are about 10 days. Given the number of shortwave and longwave infrared bands, ASTER has been popular for tracking volcanic activity worldwide (Ramsey & Dehn 2004; Carter *et al.* 2008; Vaughan *et al.* 2008; Surono *et al.* 2012; Delgado *et al.* 2014).

ASTER data are normally available after a day or more wait via US Geological Survey (USGS) Earth Explorer, but expedited ASTER data for Hawaiʻi are processed under the ASTER URP (urgent request protocol; Ramsey *et al.* 2004). The URP is a system that provides low-latency ASTER data for a select number of locations on Earth. We have a Matlab script that scans the ASTER URP FTP site, reading the metadata files to identify new scenes which cover Hawaiʻi. The script downloads the ASTER image and warps the Band 14 (11 μm) channel to a UTM projection for display. The script then exports the image as a simple JPEG which is posted on the internal HVO webserver (Fig. 2c). The Matlab script which checks the FTP site is run every few hours via Windows Scheduler.

EO-1 ALI

The NASA EO-1 (Earth Observing 1) satellite carries several sensors, one of which is ALI (Advanced Land Imager; Bicknell *et al.* 1999). ALI has 10 bands ranging from visible to shortwave infrared, nine of which have a pixel size of 30 m. In addition, a panchromatic band has a pixel size of 10 m. Band 10, at 2 μm, is the most effective band on ALI for identifying active lava. Over Hawaiʻi, acquisitions during 2013 and 2014 averaged once per week. Around the world, EO-1 ALI images have been useful for tracking volcanic activity in a variety of settings (e.g. Davies *et al.* 2006; Patrick & Smellie 2013). EO-1 ALI data are usually available on the USGS Earth Explorer website a day or more after acquisition, but the EO-1 Autonomous Sciencecraft Experiment – created by NASA-JPL (Chien *et al.* 2005) and incorporated into the NASA Volcano Sensor Web (Davies *et al.* 2013) – provides expedited data for select areas, including Kīlauea Volcano. These expedited data are available within a few hours of acquisition and are extremely useful for monitoring activity on the Puʻu ʻŌʻō flow field. We have a Matlab script, run every 2 h by Windows Scheduler, which reads the EO-1 Autonomous Sciencecraft Experiment website to identify new images. If a new image is available, the script then follows the appropriate link for image downloading. Once the image is downloaded, the script unpacks the tar (tape archive) file and opens the HDF (Hierarchical Data Format) file. The script then creates an RGB JPEG image consisting of Bands 10, 8 and 9. In this case, active breakouts – which have high values in Band 10 data – appear conspicuously as bright red in the RGB composite image (Fig. 2d). The JPEG images are posted on the HVO internal webserver for viewing.

Example application: the Kahaualeʻa 2 lava flow

Background

The Kahaualeʻa 2 flow, active between May 2013 and June 2014, was unusual in that it advanced north of Kīlauea's East Rift Zone, towards the north and NE (Fig. 3a). Other instances of NE-directed flows include (1) brief ʻaʻā flows produced by high fountaining in the early stages of Puʻu ʻŌʻō in the 1980s (Wolfe *et al.* 1988), (2) a flow that migrated NE in 2007 (Kauahikaua 2007), and (3) the original Kahaualeʻa flow that was active between January and April of 2013. The Kahaualeʻa 2 flow, however, was the longest duration active flow north of the rift zone during the Puʻu ʻŌʻō eruption.

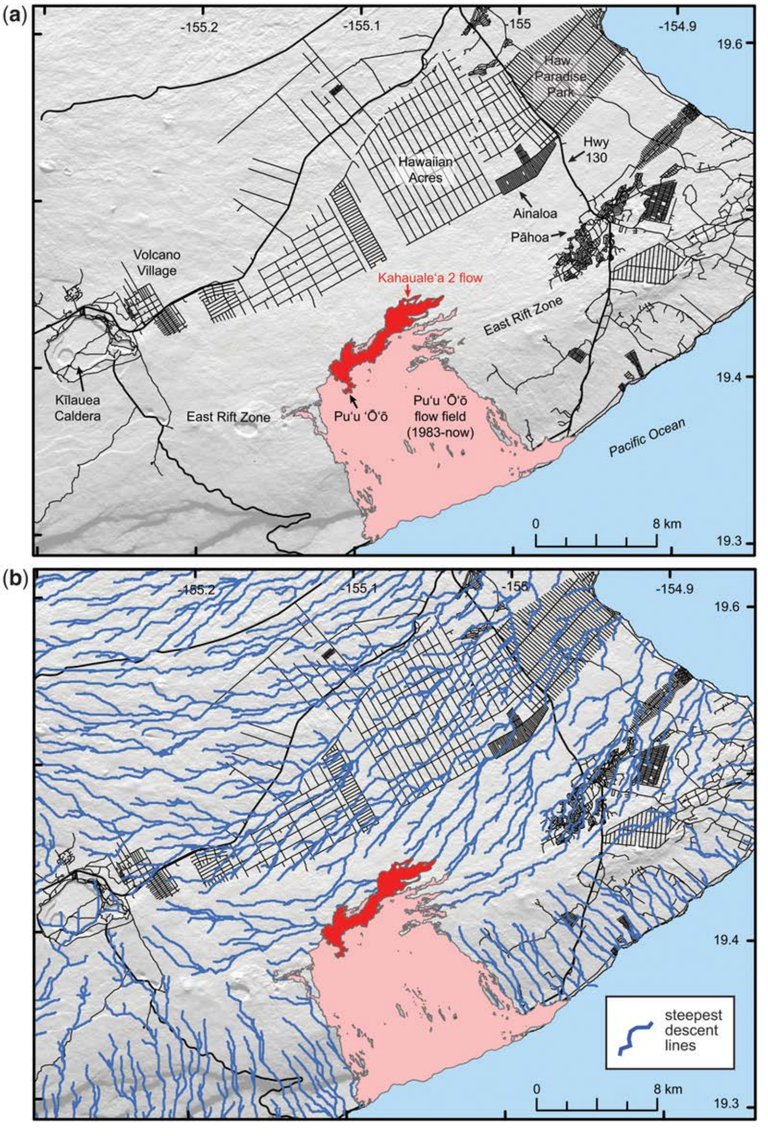

Fig. 3. (**a**) Shaded relief map of the southeastern portion of Hawaiʻi Island, covering the summit and much of the East Rift Zone of Kīlauea Volcano. The Puʻu ʻŌʻō lava flow field has been emplaced since the eruption began in 1983, and had covered 126 km^2 by 2013 (map shows flow field in mid-2014). The flow field consists of numerous individual flow units; the focus of this study is the Kahauleʻa 2 flow (2013–2014). Most flows since 1983 have travelled from vents on the East Rift Zone south towards the SE coast. The Kahauleʻa 2 flow travelled north of the rift zone, which is unusual and threatened downslope subdivisions. (**b**) Same area as in (**a**), but with steepest descent lines mapped. The steepest descent lines are used to roughly estimate the potential downslope paths of ongoing lava flow activity. The map shows that the Kahauleʻa 2 flow lies upslope of residential subdivisions including Ainaloa and Hawaiian Paradise Park.

This position put the flow upslope of several large residential subdivisions. Based on steepest descent line analysis as described in Kauahikaua (2007), the flow was upslope of subdivisions including Ainaloa (2010 Census population 2965; factfinder.census.gov) and Hawaiian Paradise Park (2010 Census population 11 404; factfinder.census.gov), as well as the main highway (Highway 130) that services the lower Puna district. If the flow were to cross Highway 130 and render it impassible, it would severely impact residents throughout lower Puna for two reasons. First, electrical utilities run along Highway 130, meaning that electrical power could be cut off for that area of the island. Second, there is no other major road that services lower Puna. Access to lower Puna from the west via Highway 130 was cut off when flows from Puʻu ʻŌʻō crossed the road in 1987 (Heliker & Mattox 2003). Although the flow remained far from residential subdivisions, residents in the Puna district were often reminded of its presence when smoke from brush fires around the flow margins was carried into residential areas. In February 2014, Hawaiʻi County Civil Defense and the Hawaiian Volcano Observatory were invited to participate in a community meeting to provide information to concerned residents. The potential hazard of the Kahaualeʻa 2 ceased when a new breakout occurred on the NE flank of Puʻu ʻŌʻō on 27 June 2014, shutting down the lava supply to the Kahaualeʻa 2 flow.

Monitoring

Satellite imagery played a critical role in monitoring the evolution of the Kahaualeʻa 2 flow and assessing its hazards. The flow front was often in remote forest and could only be reasonably accessed by helicopter, and overflights during 2013 and 2014 occurred on average once every 2 weeks. During the interim periods, satellite imagery was the primary source of information on flow front position and vigour. The GOES, MODIS, ASTER and EO-1 ALI data were each used in a manner suited to their spatial and temporal resolution. GOES data were useful in confirming that surface breakouts were active on the Kahaualeʻa 2 flow, and were also used to roughly gauge whether episodes of summit deflation, which have a tendency to diminish lava supply rates (Orr *et al.* 2014), were affecting the activity levels on the flow. This was done by qualitatively judging the rough intensity of the GOES thermal anomaly, but also by checking the automated temperature tracking product. GOES data were too coarse to make any useful measurements of flow front position. MODIS data were also used to confirm activity on the flow field in a similar manner. The 1 km pixel size also allowed very rough positioning of the active flow front. ASTER and ALI data were essential for tracking the flow front position through time, and added considerable data on flow advancement to the biweekly field mapping results. In summary we used the data together – GOES and MODIS to determine if the flow was still active, and ASTER and EO-1 ALI to track the movement of the flow front – to help fill in long (2 week) observational gaps between field visits.

A chronology of the Kahaualeʻa 2 flow can be constructed based on webcam images, overflights and EO-1 images. The Kahaualeʻa 2 lava flow began on 6 May 2013, as a NE-trending overflow from Puʻu ʻŌʻō crater (Fig. 4a), originating from a small lava pond near the eastern rim of the crater. The flow travelled rapidly down the north flank of the cone over the first few days, slowing as it reached the shallower gradient at the base of the cone. The pāhoehoe flow remained active in the flat areas north of the cone for weeks, enlarging in area as scattered breakouts gradually expanded the flow margins. In June, the flow front reached the forest, at the margin of the existing Puʻu ʻŌʻō flow field, triggering small brush fires. By August, the flow had begun to migrate slowly east (Fig. 4b), following the northern margin of the original Kahaualeʻa flow (which had been active in the same area between January and April 2013). In September, the flow front had reached the NE margin of the Puʻu ʻŌʻō flow field, and again entered forest (Fig. 4c), triggering brush fires (Fig. 5). A brief decrease in activity in mid-November caused the flow front to stall, with activity resuming about 1.4 km behind the flow front. These new breakouts eventually passed the stalled flow front in December and continued expanding into the forest (Fig. 5). A major deflation event at the summit of Kīlauea in January 2014, related to a deflation-inflation cycle (Anderson *et al.* 2015), resulted in another reduction in activity and retreat of the position of the active flows behind the flow front. This pattern of ‘two steps forward, one step back’, of the active flow front occurred several more times during the next few months, resulting in only modest overall advancement of the flow (Fig. 6). The flow front reached 8.8 km distance from the vent on Puʻu ʻŌʻō (measured as a straight line) by mid-May, followed by an abrupt step back of breakouts more than 2 km owing to a large deflation event at the summit in mid-May. By late June, 2014, active breakouts were approximately 7.1 km straight-line distance from the vent.

On 27 June 2014, a new breakout occurred on the NE flank of Puʻu ʻŌʻō cone. The new flow caused the lava level in Puʻu ʻŌʻō crater to drop, which resulted in lava at the vent area for the Kahaualeʻa 2 flow to drop approximately 7 m. The vent area consisted of a small lava pond, which fed lava into

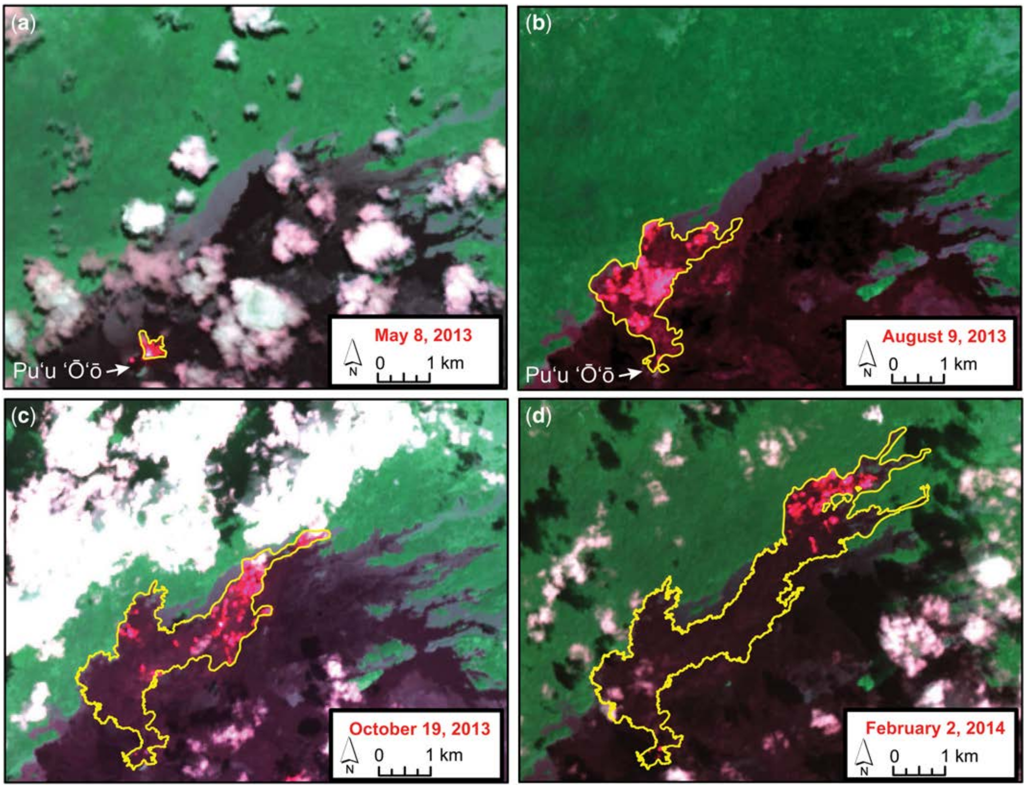

Fig. 4. Advance of the Kahauale'a 2 flow as shown by EO-1 ALI images. The images are Band 10-8-9 RGB composite images, with active surface flows showing up as bright red pixels owing to the strong Band 10 (2 μm) signal. The Kahauale'a 2 flow field outline, based on field mapping and satellite images, is shown by the yellow line. (**a**) The flow began on 6 May 2013, and just 2 days later the flow was still travelling down the flanks of Pu'u 'Ō'ō cone, with high temperatures over most of the flow surface. (**b**) Three months later, in early August, the flow had travelled north to reach the forest boundary. At this point, active breakouts were limited to patches across the flow surface, presumably owing to a nascent tube system evolving beneath the crust. (**c**) By mid-October, flows had travelled 5.6 km NE of the vent. At this time, most of the breakouts were limited to the distal half of the flow, indicating a maturing lava tube in the proximal half. (**d**) During 2014, nearly all breakouts were limited to an area at the distal end of the flow, implying a mature tube carrying lava from the vent to the flow front.

the entrance of the lava tube. The drop in lava level at this pond resulted in lava dropping below the elevation of the tube entrance, abruptly cutting off lava supply to the Kahauale'a 2 flow. Residual lava in the tube system trickled out on the surface over the next few days, but all surface flows on the Kahauale'a 2 flow had ceased by 30 June 2014.

During typical activity on the Kahauale'a 2 flow during 2014, surface activity consisted of scattered pāhoehoe lobes limited to the distal end of the Kahauale'a 2 flow field, shown clearly by EO-1 images (Fig. 7a). In many cases, these surface breakouts were more than 5 km from the vent. The absence of surface flows in the intervening span implied an efficient lava tube supplying lava from the vent to the active breakouts. This tube, which consisted of a single master tube for much of its length, was roughly mapped (Fig. 7a) by marking the trace of small fuming sources, assisted by images from a handheld thermal camera. When the 27 June 2014 breakout occurred and abruptly dropped the lava level at the vent, as mentioned above, a small collapse in the lava pond at the vent exposed the tube entrance (Fig. 7b, c). The lava tube entrance was circular in cross-section with a diameter of about 2 m (Fig. 7c). Mature lava tubes are remarkable insulators (Kauahikaua *et al.* 2003), with Helz *et al.* (2003) measuring temperature drops of $\leq 10^{\circ}C$ in lava flowing through 12 km of a lava tube. Recognizing a well-established lava tube on the Kahauale'a 2 flow was therefore an important part of HVO's hazard assessment, as lava tubes

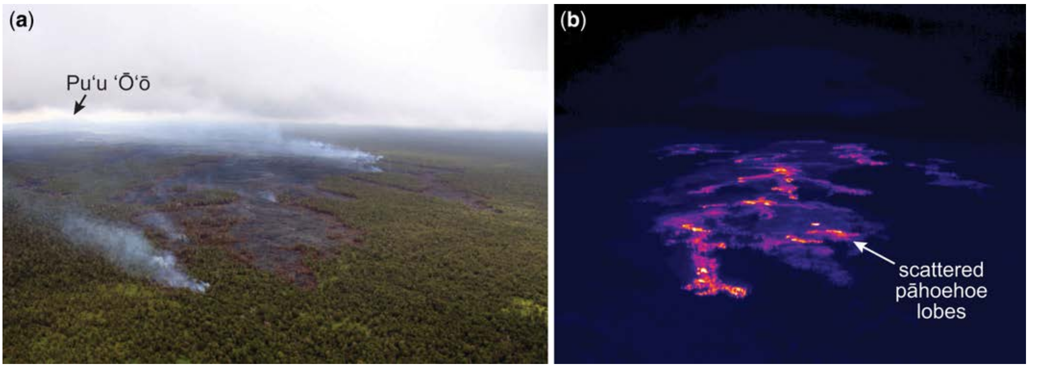

Fig. 5. Visual and thermal views of the Kahauale'a 2 flow front from the helicopter, taken 18 April 2014. (**a**) Photograph showing several smoke plumes originating from brush fires at the margin of the flow. Note Pu'u 'Ō'ō, where the vent is situated, in the upper left. (**b**) Thermal camera image taken at same time, showing the scattered nature of surface activity on the flow field. The surface flows consist of numerous lobes of slowly moving pāhoehoe. Active pāhoehoe is shown by white and yellow colours.

allow even low-effusion-rate flows to travel long distances.

Compiling the flow front data from both helicopter overflights and satellite imagery, a detailed plot of the flow front position through time has been constructed (Fig. 6). The overall average advance rate, measured as a straight line between the vent on Pu'u 'Ō'ō and the active flow front, was 17 m/day (or 18.7 m/day as measured along the flow centreline). Higher advance rates were present at the start of the flow as it travelled down the steep flanks of Pu'u 'Ō'ō, as well as when the flow was confined (and therefore focused) along the margin of the original Kahauale'a flow and the flank of a perched lava

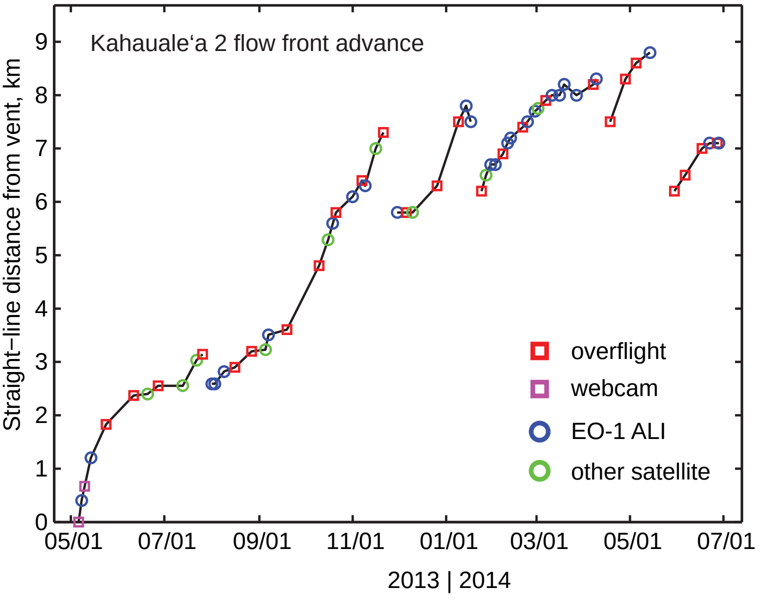

Fig. 6. Advance of the Kahauale'a 2 lava flow, erupting from Kīlauea's East Rift Zone, during 2013–2014. Distances shown are straight-line measurements between the active flow front and the vent on Pu'u 'Ō'ō. Along-flow measurements of advance in this case add about 10% to the distances shown here. Measurements of the flow advance originate primarily from biweekly overflights and satellite imagery (such as EO-1 ALI images). Several interruptions in lava supply (mid-November 2013, mid-January 2014, April and May 2014) caused the flow front to stall, with active breakouts persisting or reappearing some distance behind the stalled flow front.

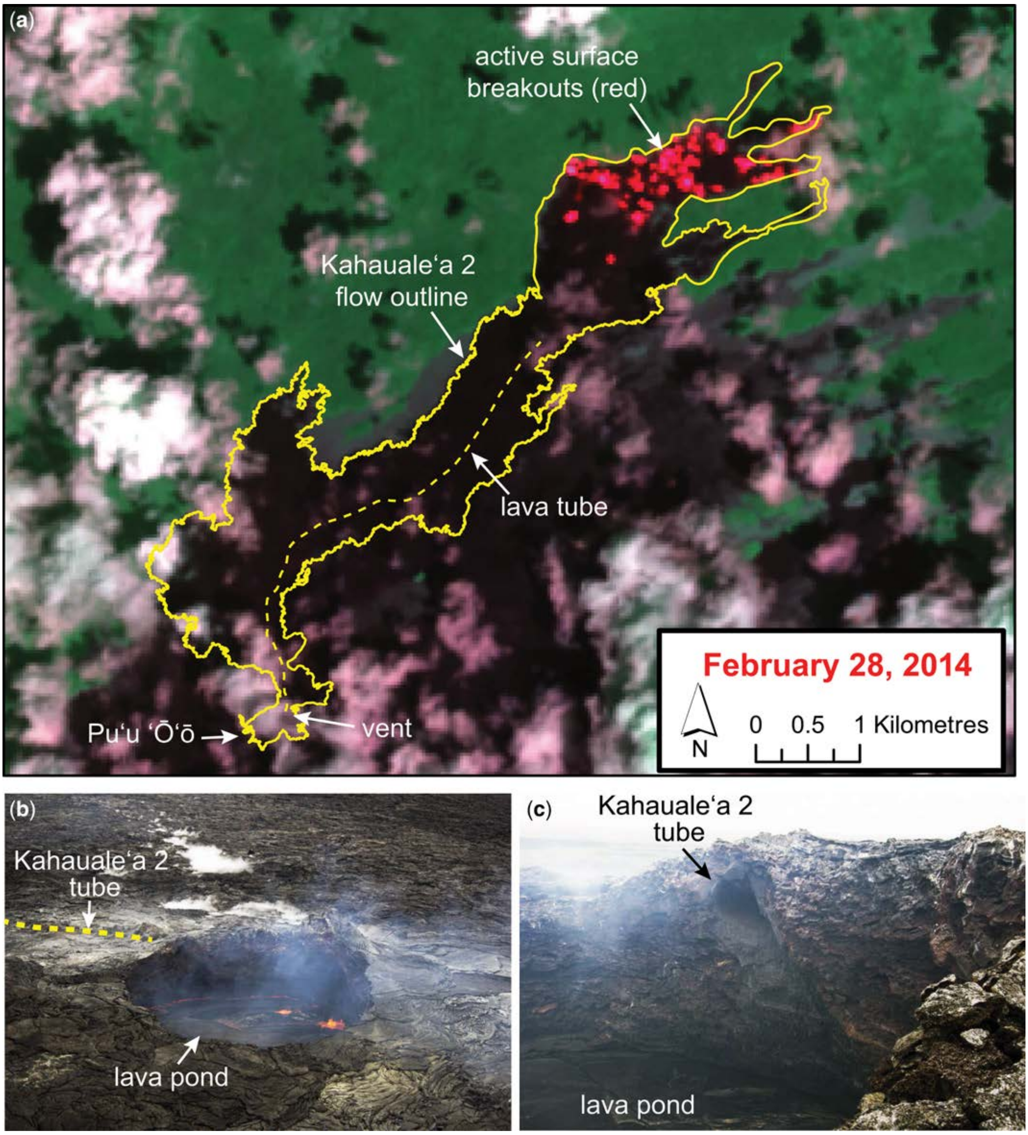

Fig. 7. (**a**) Typical view of Kahauale'a 2 flow with EO-1 ALI. During much of the life of the Kahauale'a 2 flow, active breakouts were limited to the distal end of the flow (in this case, at a distance of more than 5 km from the vent on Pu'u 'Ō'ō). This distance implies a lava tube supplying lava to the distal end of the flow. The dotted line shows the rough path of this lava tube, based on field mapping of fume sources and elevated surface temperatures in thermal camera imagery. The active breakouts (red) consist of scattered, slowly moving pāhoehoe lobes (Fig. 5). (**b**) View of the lava pond, at Pu'u 'Ō'ō , at the vent area (marked in part 'a' above) for the Kahauale'a 2 flow. The lava tube supplying the flow begins at this spot. The lava pond dropped on 27 June 2014, cutting off the flow of lava into the tube, and terminated the Kahauale'a 2 flow. For scale, the pond is 35 m in diameter. Photograph taken 30 June 2014. (**c**) View of the tube entrance from the rim above the lava pond. The tube is about 2 m in diameter here. Photograph taken 30 June 2014.

channel from late 2007 (Patrick *et al.* 2011). Apparent negative advance rates of the active front occurred during abrupt decreases in activity, when surface flows at the flow front would stall. The surface flows that persisted during, or reappeared following, these interruptions were positioned hundreds of metres behind the former flow front, creating a 'retreat' in surface flow position. Several abrupt decreases in lava supply such as this occurred as a result of deflation–inflation events at Kīlauea's summit (Orr *et al.* 2014; Anderson *et al.* 2015). This erratic and unsteady advancement is a testament not only to the effects of local topography on flow advancement, but also to the importance of short-term lava supply rate changes in pāhoehoe flow field evolution. Even between episodes of lava supply interruption, the flow advance rate was low (e.g. 28 m/day during February and March 2014), probably owing to a combination of the low slope north of the rift zone (approximately 1.7° near the Kahauale'a 2 flow front), and the low effusion rate. Preliminary estimates of the time-averaged discharge rate for the Kahauale'a 2 flow are 1–3 $m^3\,s^{-1}$ (M. Poland, pers. comm., using the technique of Poland 2014), which is half, or less, than typical rates measured by Sutton *et al.* (2003) for the eruption (see also Patrick *et al.* (2011), which stated an effusion rate of $6 \pm 2\ m^3\,s^{-1}$ for late 2007 activity, based on the methods of Sutton *et al.* (2003)).

Hazard assessment

One of the first questions in a lava flow hazard scenario is 'Where is the lava heading?' To answer this we follow the general approach described by Kauahikaua (2007), which described hazards related to a 2007 flow that was active in the same general area as the Kahauale'a 2 flow. Kauahikaua (2007) relied primarily on the map of the current flow front position along with the map of steepest descent lines to anticipate roughly where the flow front would advance downslope. The steepest descent lines depict hydraulic drainage paths, and have compared well with the paths of actual lava flows (Kauahikaua 2007). Figure 3b shows the map of steepest descent lines calculated with ArcGIS from a 10 m US Geological Survey digital elevation model from 1983, created from digitized contours. As the map shows, the steepest descent lines extending from the front of the Kahauale'a 2 flow continue NE and enter the Ainaloa subdivision, crossing Highway 130 NW of the town of Pāhoa, and then continue through the eastern portion of Hawaiian Paradise Park to reach the ocean.

Once a general idea is established of the areas downslope that may potentially be threatened, the next question is 'How long will it take the lava to get there?' To answer this we take an empirical approach and focus on the observed advance rates of the flow, rather than using theoretical lava flow models. This is, in large part, due to the fact that existing lava flow models are suited to channelized 'a'ā flows (e.g. Harris & Rowland 2001) and not tube-fed pāhoehoe flows. We use the flow advance plot in Figure 6 to measure the average advance rate of the flow, and apply this rate to the remaining distance to the closest residential areas on a downslope path (Fig. 3b). The closest subdivision (Ainaloa) on a downslope path is roughly 10 km from the farthest flow front of the Kahauale'a 2. Given the average advance rate noted above (17 m/day), it would have therefore required much more than a year for the flows to reach the subdivision – assuming that the flow advance rate, and frequency of lava supply interruptions, remained similar. Given this large amount of time, it was considered possible that the vent on Pu'u 'Ō'ō supplying lava to the Kahauale'a 2 flow might destabilize and shut down, or produce lava flows in another direction, within that timeframe. The vent supplying lava to the Kahauale'a 2 flow did, indeed, shut down on 27 June 2014, as a new flow (the June 27th flow) appeared on Pu'u 'Ō'ō's NE flank.

By tracking the Kahauale'a 2 flow in a detailed manner – a task greatly assisted by satellite imagery – HVO assessed the Kahauale'a 2 flow hazard and communicated this with Hawai'i County Civil Defense (the local emergency managers) and directly to the public (via public talks and articles in the local newspapers, as well as the HVO website). The information above was distilled into several simple talking points used to communicate the hazard to the public while the Kahauale'a 2 flow was active:

(1) 'There is no immediate threat to life or property, because the flow is still far from residential areas and advancing very slowly'.
(2) 'The Kahauale'a 2 flow does have the potential to be a threat in the future, because residential areas are downslope'.
(3) 'Whether or not the flow develops into a threat depends on the eruption rate and flow advance rate in the coming months, and HVO is closely monitoring the situation'.
(4) 'Puna residents should stay informed as the situation progresses'.

The 'June 27th' flow remains active as of April 2015. During NE advancement in August and September, 2014, the flow was confined, in part, by a series of ground cracks along the East Rift Zone. In October 2014 the 27th June lava flow entered the town of Pāhoa, disrupting the lives of nearby residents and threatening to cover the main road access for communities on the eastern tip of the island (McCarter 2014). Activity on the flow field fluctuated in late 2014 and early 2015, destroying a home and partially burying a cemetery. In March 2015 the portion of the flow near Pāhoa became inactive, but active breakouts persisted upslope, closer to Pu'u 'Ō'ō, through April 2015. Observations from frequent helicopter overflights and ground mapping were augmented with satellite imagery. HVO used steepest descent path analysis, as described above, for forecasting the 27th June flow paths and communicating potential hazard scenarios with Hawai'i County Civil Defense. These expected paths compared reasonably well with actual flow paths. Additional insight on potential flow paths was provided by stochastic steepest-descent path simulations in the manner of Favalli *et al.* (2005). While potential flow paths were relatively well constrained, flow advancement rates were much more difficult to forecast, owing to fluctuations in effusion rate, influences from small-scale topography, and the complex and scattered nature of pāhoehoe flow-field development (Kauahikaua *et al.* 2003; Orr *et al.* 2014).

Future work and Mauna Loa

What we describe here is only a first step in thermal remote sensing at the Hawaiian Volcano Observatory. This nascent system automates the downloading and display of various datatypes but does little in the way of analyses. To truly reduce the lag time between image acquisition and hazard assessment, automated analyses and forecasting need to be established. This planned system might emulate that developed by Italy's INGV (Istituto Nazionale di Geofisica e Vulcanologia) for monitoring Mount Etna (Ganci *et al.* 2011, 2012). That system has three main components:

(1) hotspot detection;
(2) effusion rate estimation;
(3) lava flow forecasting.

Each of these elements could be useful for monitoring Hawaiian volcanoes. Hotspot detection, in the manner of either Ganci *et al.* (2011) or Wright *et al.* (2004), could be applied to GOES and MODIS data. Hotspot detection in GOES data would provide a particularly rapid indication of new activity. Effusion rate estimates, based on the size and temperature of the detected hotspots, can be done using the technique of Harris *et al.* (1997*b*). This would provide a first-order estimate of eruption vigour, and be useful in the initial stages of activity when field data may not yet be available. Forecasting the path and distance of lava flows can then be done using existing models, using the geographic coordinates of the detected hotspots as a starting location. These dynamic models, however, normally assume a single, channelized flow (e.g. Harris & Rowland 2001). Whereas this may be relevant for the activity on Mauna Loa or future high lava fountaining events on Kīlauea, the current flows on Kīlauea are predominantly pāhoehoe, which has very different flow behaviour (Kauahikaua *et al.* 2003). Therefore, for Kīlauea under current eruptive conditions, we may forgo models that attempt to forecast lava flow distance and instead focus on automated analyses of potential downslope paths, which would be more broadly applicable for the range of behaviour (i.e. both 'a'ā and pāhoehoe) we observe. Favalli *et al.* (2005) take a stochastic approach to modelling downslope paths, running thousands of iterations of downslope migration and adding noise across the digital elevation model at each run – in effect considering the inherent uncertainty in the digital elevation model to produce an envelope of downslope paths. We have used this approach in a preliminary manner with good results in Hawai'i.

These improvements should prove critical for monitoring any future activity at Mauna Loa. We can envision how the system might work during the next eruption.

In a hypothetical scenario:

> Months of increasing seismic activity and inflation at the summit of Mauna Loa have HVO scientists on high alert and the volcano on alert level WATCH. The first appearance of lava at the surface occurs at night, on the floor of Mauna Loa's summit caldera (Moku'āweoweo) as a line of lava fountains. This fountaining sets off an automated alarm system on the current thermal camera operating at the summit (Patrick *et al.* 2014) sending a text message to HVO scientists. Within minutes, this activity also produces an intense thermal anomaly in GOES imagery, and the hotspot detection routine identifies this and also sends a text message to HVO staff – helping to confirm the new activity. The system then makes a preliminary estimate of effusion rate, which is a minimum estimate as the fountaining has saturated the GOES pixels. Refined estimates of effusion rate are then available within hours using the next MODIS pass. The flows remain contained within the summit caldera and pose no hazard to downslope communities, and the effusion dies out after several weeks, ending the summit eruption.
>
> Summit eruptions are commonly followed by rift zone eruptions on Mauna Loa (Macdonald *et al.* 1983), and these rift eruptions pose greater potential hazard to residential areas downslope. Months after the hypothetical summit eruption described above, lava begins erupting from one of Mauna Loa's rift zones as a long line of fountaining, again in the middle of the night. Our thermal cameras do not currently cover the rift zones, so no alarm is possible from that system, but the intense hotspot is detected in GOES imagery within minutes, sending a text alert to HVO staff. Seismic tremor alarms also begin sending out alerts to staff. A preliminary estimate is made of effusion rate, which is again a minimum value owing to the saturated pixels. An improved estimate is made in the early morning values using MODIS, at which time field geologists have begun helicopter overflight operations and field estimates of eruption rate (Lipman & Banks 1987; Harris *et al.* 2007). The automated system then produces a map of potential downslope paths using the detected hotspots as starting coordinates, producing a preliminary map of areas susceptible to future

inundation. HVO geologists then integrate this map, along with the satellite-derived and field-based effusion rates to construct an initial hazard assessment that is communicated to Hawai'i County Civil Defense. Civil Defense then uses this information for ongoing emergency notifications and evacuations.

Many of these improvements were implemented in a preliminary manner in April 2015, and are currently being tested. A GOES alert scheme detects hotspots and automatically sends out a text message to HVO staff if the hotspot is located on Mauna Loa. MODIS data are alarmed using the MODVOLC approach (Wright *et al.* 2004) to detect hotpots, and alerts are also sent via text message. Initial estimates of radiant heat flux are calculated using the approach of Wright & Flynn (2004), and used to make estimates of effusion rate. The coordinates of the hotspot are used as an input to an automated stochastic simulation of steepest descent paths, in the manner of Favalli *et al.* (2005).

Future satellite sensors should allow improved spatial, spectral and temporal monitoring of volcanic activity in Hawai'i. The GOES-R Advanced Baseline Imager will have a pixel size of 2 km for infrared bands, an increased acquisition frequency (one image every 5 min), as well as a total of 16 bands (Schmit *et al.* 2005). The improved acquisition frequency should greatly reduce the time lag of automated thermal alerts, and the improved spatial and spectral resolution should allow more accurate estimates of radiant heat flux and effusion rates.

Conclusions

Satellite imagery plays an important role in filling in observational gaps in Hawai'i, particularly for remote lava flows. For these data to be useful in an operational environment, the acquisition and processing must be automated to produce a finished product for observatory staff. At HVO, we have the first stages of a system to acquire and process satellite imagery, including GOES, MODIS, ASTER and EO-1 ALI. Because HVO currently lacks access to a ground receiving station, we utilize existing internet sources which have low latency (i.e. no more than several hours between acquisition and availability). These data have proven useful for monitoring lava flow activity on Kīlauea's East Rift Zone. A recent lava flow, the Kahauale'a 2 flow, was active upslope of several residential subdivisions during 2013–2014. Satellite imagery contributed greatly to monitoring the advance of the flow and assessing its ongoing hazards. Ongoing improvements to this system include automated hotspot detection, effusion rate estimation and flow forecasting – all of which would be useful for monitoring the next eruption of Mauna Loa.

We are grateful to R. Wright and E. Pilger (University of Hawaii Manoa), who assisted HVO with an early version of the MODIS acquisition approach. Loren Antolik and Lopaka Lee (HVO) are thanked for maintaining the internal webserver and computer systems. Pilot David Okita was essential to the success of airborne mapping and monitoring of the Kahauale'a 2 flow. Reviews by R. Wright, S. Carn and R. Wessels are appreciated. The Matlab code written for satellite image downloading and analysis is freely available upon request (mpatrick@usgs.gov). Any use of trade, firm or product names is for descriptive purposes only and does not imply endorsement by the US Government.

References

Amelung, F., Yun, S.-H., Walter, T. R., Segall, P. & Kim, S.-W. 2007. Stress control of deep rift intrusion at Mauna Loa Volcano, Hawaii. *Science*, **316**, 1026–1030, http://doi.org/10.1126/science.1140035

Anderson, K., Poland, M., Johnson, J. & Miklius, A. 2015. Episodic deflation-inflation events at Kilauea Volano and implications for the shallow magma system. *In*: Carey, R., Poland, M., Cayol, V., Weis, D. (eds) *Hawaiian Volcanism: From Source to Surface*. American Geophysical Union, Geophysical Monograph, Wiley, Hoboken, NJ, **208**, 229–250.

Barnes, W. L., Pagano, T. S. & Salomonson, V. V. 1998. Prelaunch characteristics of the Moderate Resolution Imaging Spectroradiometer (MODIS) on EOS-AMI. *IEEE Transactions on Geosciences and Remote Sensing*, **36**, 1088–1100.

Bicknell, W. E., Digenis, C. J., Forman, S. E. & Lencioni, D. E. 1999. EO-1 advanced land imager. *In*: *Proceedings of SPIE 3750, Earth Observing Systems IV*, **80**, 24 September 1999, http://doi.org/10.1117/12.363501

Carter, A. J., Girina, O., Ramsey, M. S. & Demyanchuk, Y. V. 2008. ASTER and field observations of the 24 December 2006 eruption of Bezymianny Volcano, Russia. *Remote Sensing of Environment*, **112**, 2569–2577, http://doi.org/10.1126/science.1140035

Chien, S., Sherwood, R. *et al.* 2005. Using autonomy flight software to improve science return on earth observing one. *Journal of Aerospace Computing, Information and Communication*, **2**, 196–216.

Davies, A. G., Chien, S., Baker, V. *et al.* 2006. Monitoring active volcanism with the Autonomous Sciencecraft experiment on EO-1. *Remote Sensing of Environment*, **101**, 427–446, http://doi.org/10.1016/j.rse.2005.08.007

Davies, A. G., Chien, S. *et al.* 2013. Observing Iceland's Eyjafjallajökull 2010 eruptions with the autonomous NASA Volcano Sensor Web. *Journal of Geophysical Research*, **118**, 1–21, http://doi.org/10.1002/jgrb.50141

Delgado, F., Pritchard, M., Lohman, R. & Naranjo, J. A. 2014. The 2011 Hudson volcano eruption (Southern Andes, Chile): pre-eruptive inflation and hotspots observed with InSAR and thermal imagery. *Bulletin of Volcanology*, **76**, 815, http://doi.org/10.1007/s00445-014-0815-9

Favalli, M., Pareschi, M. T., Neri, A. & Isola, I. 2005. Forecasting lava flow paths by a stochastic approach. *Geophysical Research Letters*, **32**, L03305, http://doi.org/10.1029/2004GL021718

Flynn, L. P., Mouginis-Mark, P. J. & Horton, K. A. 1994. Distribution of thermal areas on active lava flow field: landsat observations of Kīlauea Volcano, Hawaii, July 1991. *Bulletin of Volcanology*, **56**, 284–296.

Ganci, G., Vicari, A., Fortuna, L. & Del Negro, C. 2011. The HOTSAT volcano monitoring system based on combined use of SEVIRI and MODIS multispectral data. *Annals of Geophysics*, **54**, 544–550.

Ganci, G., Vicari, A., Cappello, A. & Del Negro, C. 2012. An emergent strategy for volcano hazard assessment: from thermal satellite monitoring to lava flow modeling. *Remote Sensing of Environment*, **119**, 197–207, http://doi.org/10.1016/j.rse.2011.12.021

Gawarecki, S. J., Lyon, R. J. P. & Nordberg, W. 1965. Infrared spectral returns and imagery of the Earth from space and their application to geologic problems. *American Astronomical Society Science and Technology Series*, **4**, 13–33.

Guffanti, M., Diefenbach, A. K., Ewert, J. W., Ramsey, D. W., Cervelli, P. F. & Schilling, S. P. 2009. *Volcano-monitoring instrumentation in the United States, 2008*. US Geological Survey Open-File Report **2009-1165**.

Harris, A. J. L. 2013. *Thermal Remote Sensing of Active Volcanoes: A User's Manual*. Cambridge University Press, New York.

Harris, A. J. L. & Ripepe, M. 2007. Regional earthquake as a trigger for enhanced volcanic activity: evidence from MODIS thermal data. *Geophysical Research Letters*, **34**, L02304, http://doi.org/10.1029/2006GL028251

Harris, A. J. L. & Rowland, S. K. 2001. FLOWGO: a kinematic therm-rheological model for lava flowing in a channel. *Bulletin of Volcanology*, **63**, 20–44.

Harris, A. J. L. & Thornber, C. R. 1999. Complex effusive events at Kīlauea as documented by the GOES satellite and remote video cameras. *Bulletin of Volcanology*, **61**, 382–395.

Harris, A. J. L., Keszthelyi, L. P. *et al.* 1997*a*. Chronology of the episode 54 eruption at Kīlauea Volcano, Hawaii, from GOES-9 satellite data. *Geophysical Research Letters*, **24**, 3281–3284.

Harris, A. J. L., Blake, S., Rothery, D. A. & Stevens, N. F. 1997*b*. A chronology of the 1991 to 1993 Mount Etna eruption using advanced very high resolution radiometer data: implications for real-time thermal volcano monitoring. *Geophysical Research Letters*, **102**, 7985–8003.

Harris, A. J. L., Flynn, L. P., Keszthelyi, L. P., Mouginis-Mark, P. J., Rowland, S. K. & Resing, J. A. 1998. Calculation of lava effusion rates from Landsat TM data. *Bulletin of Volcanology*, **60**, 52–71.

Harris, A. J. L., Pilger, E., Flynn, L. P., Garbeil, H., Mouginis-Mark, P. J., Kauahikaua, J. & Thornber, C. 2001. Automated, high temporal resolution, thermal analysis of Kīlauea volcano, Hawai'i, using GOES satellite data. *International Journal of Remote Sensing*, **22**, 945–967.

Harris, A. J. L., Dehn, J. & Calvari, S. 2007. Lava effusion rate definition and measurement: a review. *Bulletin of Volcanology*, **70**, 1–22, http://doi.org/10.1007/s00445-007-0120-y

Heliker, C. & Mattox, T. N. 2003. The first two decades of the Pu'u 'Ō'ō–Kupaianaha eruption: chronology and selected bibliography. *In*: Heliker, C., Swanson, D. A. & Takahashi, T. J. (eds) *The Pu'u 'Ō'ō–Kupaianaha Eruption of Kīlauea Volcano, Hawai'i: The First 20 Years*. US Geological Survey, Reston, Virginia, Professional Paper, **1676**, 1–27.

Helz, R. T., Heliker, C., Hon, K. & Mangan, M. 2003. Thermal efficiency of lava tubes in the Pu'u 'Ō'ō -Kupaianaha eruption. *In*: Heliker, C., Swanson, D. A. & Takahashi, T. J. (eds) *The Pu'u 'Ō'ō–Kupaianaha Eruption of Kīlauea Volcano, Hawai'i: The First 20 Years*. US Geological Survey, Professional Paper, **1676**, 105–120.

Jaggar, T. A. 1930. The Hualalai earthquake crisis of 1929. The Volcano Letter, no. 309. Reprinted as: Fiske, R. S., Simkin, T., Nielson, A. (eds) 1987. *The Volcano Letter*. Smithsonian Institution Press, Washington, DC.

Kauahikaua, J. 2007. *Lava flow hazard assessment, as of August 2007, for Kīlauea East Rift Zone eruptions, Hawai'i Island*. US Geological Survey Open-File Report 2007-1264

Kauahikaua, J., Cashman, K., Clague, D., Champion, D. & Hagstrum, J. 2002. Emplacement of the most recent lava flows on Hualālai Volcano, Hawai'i. *Bulletin of Volcanology*, **64**, 229–253.

Kauahikaua, J., Sherrod, D. R., Cashman, K. V., Heliker, C., Hon, K., Mattox, T. N. & Johnson, J. A. 2003. Hawaiian lava flow dynamics during the Pu'u 'Ō'ō -Kupaianaha eruption: a tale of two decades. *In*: Heliker, C., Swanson, D. A. & Takahashi, T. J. (eds) *The Pu'u 'Ō'ō–Kupaianaha Eruption of Kīlauea Volcano, Hawai'i: The First 20 Years*. US Geological Survey, Professional Paper, **1676**, 63–88.

Kervyn, M., Ernst, G. G. J. *et al.* 2008. Voluminous lava flows at Oldoinyo Lengai in 2006: chronology of events and insights into the shallow magmatic system. *Bulletin of Volcanology*, **70**, 1069–1086, http://doi.org/10.1007/s00445-007-0190-x

Koeppen, W. C., Pilger, E. & Wright, R. 2011. Time series analysis of infrared satellite data for detecting thermal anomalies: a hybrid approach. *Bulletin of Volcanology*, **73**, 577–593, http://doi.org/10.1007/s00445-010-0427-y

Koeppen, W. C., Patrick, M., Orr, T., Sutton, A. J., Dow, D. & Wright, R. 2013. Constraints on the partitioning of Kīlauea's lava between surface and tube flows, estimated from infrared satellite data, sulfur dioxide emission rates and field observations. *Bulletin of Volcanology*, **75**, 716, http://doi.org/10.1007/s00445-013-0716-3

Lipman, P. W. & Banks, N. G. 1987. Aa flow dynamics, Mauna Loa 1984. *In*: Decker, R. W., Wright, T. L. & Stauffer, P. H. (eds) *Volcanism in Hawaii*. US Geological Survey, Professional Paper, **1350**, 1527–1568.

Lockwood, J. P., Dvorak, J. J., English, T. T., Koyanagi, R. Y., Okamura, A. T., Summers, M. L. & Tanigawa, W. R. 1987. Mauna Loa 1974–1984: a decade of intrusive and extrusive activity. *In*: Decker, R. W., Wright, T. L. & Stauffer, P. H. (eds) *Volcanism in Hawaii*. US Geological Survey, Professional Paper, **1350**, 537–570.

Macdonald, G. A. 1954. Activity of Hawaiian volcanoes during the years 1940–1950. *Bulletin Volcanologique*, **15**, 119–179.

Macdonald, G. A., Abbot, A. T. & Peterson, F. L. 1983. *Volcanoes in the Sea: The Geology of Hawaii*, 2nd edn. University of Hawaii Press, Honolulu, HI.

McCarter, T. 2014. Scientists engage with public during lava flow threat. *Eos*, **95**, 409–410.

Miklius, A. & Cervelli, P. 2003. Vulcanology: interaction between Kīlauea and Mauna Loa. *Nature*, **421**, 229.

Miklius, A., Cervelli, P. *et al.* 2005. *Global positioning system measurements on the Island of Hawai'i: 1997 through 2004*. US Geological Survey Open-File Report **2005-1425**.

Moran, S. C., Newhall, C. & Roman, D. C. 2011. Failed magmatic eruptions: late-stage cessation of magma ascent. *Bulletin of Volcanology*, **73**, 115–122.

Orr, T. R., Heliker, C. & Patrick, M. 2013. *The ongoing Pu'u 'Ō'ō eruption of Kīlauea Volcano, Hawai'i – 30 years of eruptive activity*. US Geological Survey Fact Sheet 2012-3127.

Orr, T., Bleacher, J., Patrick, M. & Wooten, K. 2014. A sinuous elongate tumulus over an active lava tube at Kilauea Volcano: evolution, analogs, and hazard forecasts. *Journal of Volcanology and Geothermal Research*, **291**, 35–48.

Patrick, M. R. & Smellie, J. L. 2013. A spaceborne inventory of volcanic activity in Antarctica and southern oceans, 2000–10. *Antarctic Science*, **25**, 475–500, http://doi.org/10.1017/S0954102013000436

Patrick, M. R. & Witzke, C. N. 2011. *Thermal mapping of Hawaiian volcanoes with ASTER satellite data*. US Geological Survey Scientific Investigations Report 2011-5110.

Patrick, M. R., Orr, T., Wilson, D., Dow, D. & Freeman, R. 2011. Cyclic spattering, seismic tremor, and surface fluctuation within a perched lava channel, Kīlauea Volcano. *Bulletin of Volcanology*, **73**, 639–653, http://doi.org/10.1007/s00445-010-0431-2

Patrick, M. R., Orr, T., Sutton, A. J., Elias, T. & Swanson, D. 2013. *The first five years of Kīlauea's summit eruption in Halema'uma'u, 2008–2013*. US Geological Survey Fact Sheet 2013-3116

Patrick, M. R., Orr, T., Lee, L., Antolik, L. & Kamibayashi, K. 2014. Continuous monitoring of Hawaiian volcanoes with thermal cameras. *Journal of Applied Volcanology*, **3**, 1, http://doi.org/10.1186/2191-5040-3-1

Pieri, D. & Abrams, M. 2004. ASTER watches the world's volcanoes: a new paradigm for volcanological observations from orbit. *Journal of Volcanology and Geothermal Research*, **135**, 13–28.

Poland, M. P. 2014. Time-averaged discharge rate of subaerial lava at Kīlauea Volcano, Hawai'i, measured from TanDEM-X interferometry: implications for magma supply and storage during 2011–2013. *Journal of Geophysical Research*, **119**, 5464–5481.

Ramsey, M. S. & Dehn, J. 2004. Spaceborne observations of the 2008 Bezymianny, Kamchatka eruption: the integration of high-resolution ASTER data into near real-time monitoring using AVHRR. *Journal of Volcanology and Geothermal Research*, **135**, 127–146.

Ramsey, M. S., Dehn, J., Wessels, R. L., Byrnes, J., Duda, K., Maldonado, L. & Dwyer, J. 2004. The ASTER emergency scheduling system – a new project linking near-real-time satellite monitoring of disasters to the acquisition of high-resolution remote sensing data. *In*: *American Geophysical Union Fall Meeting*. San Francisco, California, 13–17 December, 2004, abstract SF23A-0026.

Rothery, D. A., Coppola, D. & Saunders, C. 2005. Analysis of volcanic activity using MODIS thermal alerts. *Bulletin of Volcanology*, **67**, 539–556, http://doi.org/10.1007/s00445-004-0393-3

Schmit, T. J., Gunshor, M. M., Menzel, W. P., Gurka, J. J., Li, J. & Bachmeier, A. S. 2005. Introducing the next-generation advanced baseline imager on GOES-R. *Bulletin of the American Meteorological Society*, **86**, 1079–1096, http://doi.org/10.1175/BAMS-86-8-1079

Surono, Jousset, P., Pallister, J. *et al.* 2012. The 2010 explosive eruption of Java's Merapi volcano – a '100 year' event. *Journal of Volcanology and Geothermal Research*, **241**, 121–135, http://doi.org/10.1016/j.jvolgeores.2012.06.018

Sutton, A. J., Elias, T. & Kauahikaua, J. 2003. Lava effusion rates for the Pu'u 'Ō'ō -Kupaianaha eruption derived from SO2 emissions and very low frequency (VLF) methods. *In*: Heliker, C., Swanson, D. A. & Takahashi, T. J. (eds) *The Pu'u 'Ō'ō–Kupaianaha Eruption of Kīlauea Volcano, Hawai'i: The First 20 Years*. US Geological Survey, Professional Paper, **1676**, 137–148.

Vaughan, R. G., Kervyn, M., Realmuto, V., Abrams, M. & Hook, S. 2008. Satellite measurements of recent volcanic activity at Oldoinyo Lengai, Tanzania. *Journal of Volcanology and Geothermal Research*, **173**, 196–206, http://doi.org/10.1016/j.jvolgeores.2008.01.028

Wolfe, E. W., Neal, C. A., Banks, N. G. & Duggin, T. J. 1988. Geologic observations and chronology of eruptive events. *In*: Wolfe, E. W. (ed.) *The Puu Oo Eruption of Kilauea Volcano, Hawaii: Episodes 1 through 20, January 3, 1983, through June 8, 1984*. US Geological Survey, Professional Paper, **1463**, 1–97.

Wright, R. & Flynn, L. P. 2004. Space-based estimate of the volcanic heat flux into the atmosphere during 2001 and 2002. *Geology*, **32**, 189–192.

Wright, R., Flynn, L., Garbeil, H., Harris, A. J. L. & Pilger, E. 2002. Automated volcanic eruption detection using MODIS. *Remote Sensing of Environment*, **82**, 135–155.

Wright, R., Flynn, L. P., Garbeil, H., Harris, A. J. L. & Pilger, E. 2004. MODVOLC: near-real-time thermal monitoring of global volcanism. *Journal of Volcanology and Geothermal Research*, **135**, 29–49.

Yamaguchi, Y., Kahle, A. B., Tsu, H., Kawakami, T. & Pniel, M. 1998. Overview of advanced spaceborne thermal emission and reflection radiometer (ASTER). *IEEE Transactions on Geoscience and Remote Sensing*, **36**, 1062–1071.